Arrieta, M.P., Sessini, V. & Peponi, L., 2017. Biodegradable poly(ester-urethane) incorporated with catechin with shape memory and antioxidant activity for food packaging. European Polymer Journal, 94, pp.111–124.

Available at https://doi.org/10.1016/j.eurpolymj.2017.06.047

Biodegradable poly(ester-urethane) incorporated with catechin with shape memory and antioxidant activity for food packaging

Arrieta M.P.[1,*], Sessini V.[1], Peponi L.[1,*]

[1] Institute of Polymer Science and Technology (ICTP-CSIC), Madrid, Spain

Corresponding authors: marrieta@ictp.csic.es*, lpeponi@ictp.csic.es*

Abstract

Biodegradable poly(ester-urethane) (PU) based on a tri-block copolymer of poly(L-lactic acid) and poly(ε-caprolactone), with shape-memory behaviour, and further loaded with catechin (Cat), as antioxidant agent, were developed with the dual objective to obtain a smart as well as an active material for food packaging purpose. Well dispersed catechin produced somewhat UV blocking effect, but slightly amber and red tonality. Catechin demonstrated positive interaction with PU matrix enhancing the interfacial adhesion and leading to a reduction in the surface wettability. The active PU composites, with thermally-activated shape memory ability at temperatures close to those required to pack thermally proceeded food (i.e.: 40 ºC), showed increased ability to recover the initial shape of the neat PU matrix. The antioxidant effectiveness of catechin released after the exposition to a fatty food simulant was proven after 10 days which represents the worst foreseeable conditions of the intended use. The disintegration process in composting conditions of the active PU-based materials was speeded up due to the catechin incorporation. The PU formulation loaded with low amount of catechin (1 wt% or 3 wt %) showed enough transparency, enhanced shape memory behaviour, improved water resistance, reduced UV-light transmission, right catechin release and effective antioxidant activity as well as appropriate disintegration in compost. Thus, active PU-Cat composites result very interesting as smart and active materials for biodegradable food packaging applications.

Key words: poly(urethane); catechin; food packaging; shape-memory; antioxidant; biodegradable.

1. Introduction

Renewable and biodegradable polymers as well as natural additives are currently considered sustainable alternatives for food packaging applications, enhancing resource efficiency and reducing environmental negative issues associated with packaging wastes after their useful life [1]. The most studied biodegradable polymers for packaging applications are poly(lactic acid) (PLA), poly(ε-caprolactone) (PCL), poly(hydroxybutyrate) (PHB), poly(butylene succinate), starch, cellulose derivatives [2], protein obtained from plants (corn zein, wheat gluten, soy or sunflower) as well as proteins obtained from animal sources (gelatin, keratin, caseinates or whey) [3]. PLA is currently the most introduced in the market due to the fact that it presents several advantages for short term food packaging such as it is approved for food contact, is high transparent and it presents similar properties to some traditionally used plastics in the food packaging industry [4, 5]. However, for film purposes PLA is highly brittle and to increase its stretchability PLA modification results necessary. An interesting approach to tune the mechanical and thermal performance of PLA, such as thermally-activated shape-memory behaviour, is to copolymerize it with PCL in the form of tri-block polymers based on PLLA-*b*-PCL-*b*-PLLA to further obtain the corresponding poly(ester-urethane) (PU) [6-9]. Additionally, composites of PLA or its copolymers loaded with natural compounds are emerging as a new viable strategy to modify the PLA properties for preparing transparent films having controlled toughness [10]. In a previous work we synthesized a PU based on PLLA-*b*-PCL-*b*-PLLA and it was further loaded with catechin (Cat). The processing performance of PU-Cat was evaluated and it was verified that low amounts of Cat, such as 1 wt% or 3 wt%, can be well dispersed into PU matrix enhancing the thermal stability of the final composites [11]. In the present research we evaluate the multifunctional properties of the previous developed PU-Cat composites as biodegradable, smart and active systems for the food packaging industry.

In the case of polyurethanes, their shape-memory properties are attributed to their phase separation morphology that depends on the chemical structure composed by the hard and the soft segments [6]. Thermally activated SMPs are formed by two active phases having a thermal transition at a determined temperature (T_{trans}) [12], the fixity phase and the switch phase [13, 14], which can be covalently attached during the synthesis [15, 16]. The switching domains, are able to respond to the temperature depending on their amorphous or crystalline nature [6, 15, 17]. Meanwhile, the fixity

phase memorizes the initial shape of the polymer. Thermally activated SMPs are gaining industrial attention due to their potential application in several fields since they offer a number of advantages such as their easy processability, low cost, softness and their versatility for easy design for specific applications [12, 13]. Particularly, in the food packaging sector SMPs can be used for heat-shrinkable packaging films, for instance for thermally processed food [18, 19].

Thermally processed food are frequently protected by means of flexible films and subsequently heat-sealed. Thus, they presents a number of potential issues in relation to contamination after they are packed, mainly related with pack integrity and incomplete sealed films [20]. For food safety concern, the film integrity is extremely important to protect the foodstuff as well as the maintenance of the food cold chain during transport and storage. The development of SMPs in the form of heat-shrinkable films gain interest for thermally processed food since they should be packed and stored at different temperatures. Therefore, the design of a SMP where the switching phase could be activated at the packing temperature and the fixity phase at the required stored temperature will provide an interesting smart material. The film will achieve a temporary shape during packing that will be retained at the storage temperature.

On the other side, the food packaging industry demands the development of advanced packaging systems and, thus, the food packaging sector is continuously developing innovative materials focusing their attention on the development of smart and active packaging. Although both, smart and active, packaging are based on deliberate interactions with the food or the food environment, they have different purposes [21]. Smart packaging monitor the condition of packaged food or the environment surrounding the food during transport and storage [21, 22]. Alternatively, active food packaging offers the possibility to incorporate additives into the packaging material instead of directly into the food. It allows reducing the use of food additives by obtaining an active material which continuous release the active compound from the packaging to the foodstuffs [23, 24]. The purpose of the active packaging is the food shelf-life extension and the food quality maintenance or even improvement [21]. In this sense, natural phenolic compounds are interesting antioxidants for the development of antioxidant active packaging systems because they are also able to protect the polymer matrices from thermo-oxidative degradation during processing [24-26], as it was recently showed for PU based on PLLA-*b*-PCL-*b*-PLLA and further loaded with catechin (PU-Cat).

In the present work the PU-Cat are proposed as antioxidant active heat-shrinkable films intended for fatty food packaging applications. Thus, in the current work, in order to address the potential use of PU-Cat as active packaging, a more detailed study concerning the feasible release of Cat from the PU matrix to the food is reported. For this purpose, the overall and specific catechin migration studies into a fatty food simulant were assayed. Whereas the antioxidant effectiveness was tested measuring the DPPH radical scavenging activity. Additionally, some functional properties with interest for food packaging such as transparency, UV-blocking effect, colour properties and surface wettability were studied. With the aim to evaluate the possibility to use these materials as smart heat-shrinkable films, thermally-activated shape memory properties were evaluated chosen 40 ºC as the maximum temperature to make the switching domains flexible, while the lower temperature chosen was 2 ºC to simulate fridge storage temperature. Finally, since these materials are intended for the biodegradable food packaging sector their disintegration under composting conditions at a laboratory-scale level was assayed.

2. Materials and Methods

2.1. Materials

L-Lactide (L-LA), hexamethylene diisocyanate (HDI), stannous octoate ($Sn(Oct)_2$), (+)-catechin hydrate (Cat), chloroform, methanol, ethanol and 1,2-dichloroethane (DCE) were purchased from Sigma-Aldrich (Spain). 2,2-diphenyl-1-picrylhydrazyl (DPPH) 95% free radical was purchased from Fluka (Buchs, Switzerland). PCL diol CAPA 2403 (Mn = 4,155 g mol^{-1}) was kindly donated by Perstorp (Sweden). All the materials employed in this work were used as received without further purification.

2.2. Synthesis of tri-block copolymer and of its poly(ester-urethane)

The poly(ester-urethane) (PU) was synthesized by condensation [27]. In brief, it start from the synthesis of a linear tri-block copolymer based on poly(L-lactic acid) and poly(ε-caprolactone) (PLLA-*b*-PCL-*b*-PLLA) (weight ratio of 50:50) obtained by the ring opening polymerization (ROP) of L-LA initiated by PCL-diol (180 ºC, for 3 h and using $Sn(Oct)_2$ as catalyst in 0.1 wt % respect to the L-LA monomer) [6]. The tri-block, PLLA-*b*-PCL-*b*-PLLA, was reacted in 2,2-dichloroethane with 1,6-hexamethylene diisocyanate (HDI) in 1:1 in moles (80 ºC for 5 h and using $Sn(Oct)_2$ as catalyst). The PU was obtained after the solvent evaporation in a glass mould by casting method at

room temperature for 24 h. The formation of the poly(ester-urethane) was followed by attenuated total reflectance (ATR) FTIR measurements conducted at room temperature with a resolution of 4 cm^{-1} and 16 accumulation scans by using a Spectrum One FTIR spectrometer (Perkin Elmer instruments). Finally, the formation of the poly(ester-urethane) was confirmed by the ^{1}H NMR spectra at 400 MHz in a Varian Mercury 400 apparatus using deuterated chloroform as solvent and spectra was referenced to the residual solvent protons at (3.15 ppm).

The obtained poly(ester-urethane) was then pelletized and dried in vacuum for 24h at ambient conditions to eliminate the traces of the solvent. For the preparation of composites, neat PU (2g) was dissolved in 10 mL of 2,2-dichloroethane adding 1wt %, 3 wt % or 5 wt % of catechin to obtain PU-Cat1, PU-Cat3 and PU-Cat5, respectively, as it was describes in a previous work [11]. The film formulations were obtained after the solvent evaporation in a glass mould (10 cm of diameter and 0.5 mm in thickness) and they were dried in vacuum (24 h at room temperature).

2.3. Characterization of PU-Cat films

2.3.1. Light transmission

The absorption spectra in the 700-240 nm region of PU based films were investigated by means of a Perkin Elmer (Lambda 35, USA) UV-VIS spectrophotometer.

2.3.2. Color properties

The film color properties were evaluated in the CIELAB colour space using a KONICA CM-3600d COLORFLEX-DIFF2, HunterLab, Hunter Associates Laboratory, Inc, (Reston, Virginia, USA). The yellowness index (*YI*) and the colour coordinates *L* (lightness), a* (red-green) and b* (yellow-blue) were determined. The instrument was calibrated with a white standard tile. Measurements were carried out in quintuplicate at random positions over the film surface. Average values for these five tests were calculated. Total color differences (ΔE) induced by catechin incorporation with respect to the neat PU, as control film, were evaluated by the Equation (1).

$$\Delta E = \sqrt{\Delta a^{*2} + \Delta b^{*2} + \Delta L^{2}} \qquad \text{(Equation 1)}$$

The L, a* and b* colourimetric coordinates of catechin powder were also measured by means of a Minolta colorimeter CR-410 Chroma Meter (Minolta Series, Tokyo, Japan).

2.3.3. Water Contact Angle

Surface wettability of PU-Cat films was studied by means of static water contact angle measurements using a standard goniometer (EasyDrop-FM140, KRÜSS GmbH, Hamburg, Germany) equipped with a camera. Five drops of distilled water (~2 μl) were randomly placed onto the film surfaces with a syringe and, after 30 s, the water contact angle (θ^o) was determined at room temperature by means of Drop Shape Analysis SW21; DSA1 software. The average values of ten measurements for each drop with a maximum standard deviation of 3 % were reported [28].

2.3.4. Differential Scanning Calorimetry

DSC experiments were performed in a DSC 2000-TA instrument under nitrogen (50 mL min^{-1}) atmosphere. Sample weights of about 4 mg were sealed in aluminum pans and were heated from room temperature to 200 ºC at a heating rate of 10 ºC min^{-1}. The main thermal properties were determined from the second heating scan: the glass transition temperature (T_g) was taken at the midpoint of heat capacity changes, the melting temperature (T_m), cold crystallization temperature (T_{cc}) and the degree of crystallinity (χ_c) of each block of the poly(ester-urethane) was calculated through Equation 2:

$$\chi_c = \mathbf{100}\ \% \times \left[\frac{\Delta H_m - \Delta H_{cc}}{\Delta H_m^c}\right] \frac{\mathbf{1}}{\mathbf{1} - W_x} \qquad \text{(Equation 2)}$$

where W_X is the fraction of component x in the copolymer, ΔH_m is the melting enthalpy, ΔH_{cc} is the cold crystallization enthalpy, and ΔH_m^c is the melting heat associated with pure crystalline material, that is 93 J g^{-1} for PLA [29] and 148 J g^{-1} for PCL [30].

2.3.5. Shape memory behaviour

Tensile and shape-memory properties were investigated by means of an Instron machine (model 3366) equipped with a 100 N load cell and a temperature chamber with liquid nitrogen for cooling. Tensile test measurements were conducted at 40 ºC using

dogbone-style samples at a crosshead speed of 200 mm·min^{-1} with an initial length of 30 mm and at least five specimens were tested for each formulation. For shape-memory assays, films were cut in a rectangular specimen of 5.2 mm width and 20 mm length. To perform thermally-activated shape memory analysis thermo-mechanical cycles were conducted. Firstly, it is necessary to heat the sample above the corresponding T_{trans} and to strain the film. In this work, PLLA represents the fix segment and PCL the switching one [8]. Thus, the temperature at which the melting of the PCL starts was selected as T_{trans}, 40 ºC to make the switching domains flexible. The material was maintained at 40 ºC for 10 min in order to allow relaxation of the polymer chains [6]. Subsequently, the samples were stretched to 50 % at a strain rate of 20 mm min^{-1} of elongation by applying a constant deformation stress. Then, maintaining the deformation, the material was cooled down to 2 ºC. Finally, to complete the cycle the applied stress is removed and to recover the original shape the films were re-heating above the T_{trans} of 40ºC. The two main parameters used to study the shape memory performance of a material are the strain fixity ratio and the strain recovery ratio. In particular, the first one indicates the ability of the material to fix the temporary shape, while the second one indicates the ability to recover its initial shape. For each number of thermo-mechanical cycle (N), both parameters are calculated accordingly with the following equations:

Strain fixity ratio

$$R\,(N)_f = \frac{\varepsilon_u(N)}{\varepsilon_m} \times 100\% \qquad \text{(Equation 3)}$$

Strain recovery ratio

$$R(N)_r = \frac{\varepsilon_m - \varepsilon_p(N)}{\varepsilon_m - \varepsilon_p(N-1)} \times 100\% \qquad \text{(Equation 4)}$$

ε_m indicated the elongation at which the shape memory ability is calculated, in this case at 50% of deformation. ε_u, indicates the temporary shape recovered after realizing the stress. ε_p indicates the permanent shape recovered upon re-heating the sample.

2.3.6. Overall and specific migration

Release studies were conducted by the determination of overall and specific migration tests into solutions of 50% v/v ethanol (simulant D1) because these materials

are intended for fatty food-packaging application [31]. Release tests were performed in triplicate by total immersion of pre-weighed samples in the food simulant D1 contained in glass tubes which were kept at 40 ºC for 10 days which are those recommended for fatty food products. After the incubation period, films were removed. In the case of the overall migration tests, after 10 days the food simulants were almost evaporated on a heating plate and then dried in an oven at 110 ºC for 30 min to get the residue, which was weighed in an analytical balance Sartorius BP211D (Goettingen, Germany) to ± 0.1 mg to determine the overall migration as mg kg^{-1} of food simulant.

Specific migration tests were also conducted in food simulant D1. The released amount of catechin into the food simulant after 10 contact days was determined by the measurement of UV absorbance at 280 nm attributed to the B ring of catechin moiety, by means of a UV-Vis Perkin Elmer (Lambda 35, USA) UV-VIS spectrophotometer.

2.3.7. Antioxidant activity

The antioxidant effectiveness of PU-Cat was measured according to DPPH-method [32] by determining the absorbance at 517 nm of release medium at different times by means of UV-Vis Perkin Elmer (Lambda 35, USA) spectrophotometer. The antioxidant activity was obtained according Equation 5:

$$I\ (\%) = \left(\frac{A_{control} - A_{sample}}{A_{control}}\right) \times 100\% \qquad \text{(Equation 5)}$$

where I (%) is the percentage of inhibition. $A_{control}$ the absorbance of DPPH in ethanolic solution and A_{sample} the absorbance of DPPH after 15 minutes in contact with each sample. The results were calculated in % of inhibition and they were expressed as the equivalent of gallic acid (GA) concentration (mg kg^{-1}) by using a calibrated curve of gallic acid concentration versus I (%).

2.3.8. Disintegration under composting conditions

The disintegration in composting conditions of films was tested at laboratory scale level according to the ISO 20200 standard [33]. Films (cut in 15 mm x 15 mm) were pre-weighted and buried at 4-6 cm depth in perforated plastic boxes containing a solid synthetic wet waste prepared with 10 % of compost (Mantillo, Spain), 30 % rabbit food, 10 % starch, 5 % sugar, 1 % urea, 4 % corn oil and 40 % sawdust and

approximately 50 wt % of water content. Film samples were then incubated at aerobic conditions at 58 ºC and further recovered at 9, 16, 28 and 44 days of disintegration, cleaned with distilled water, dried in an oven at 37 ºC during 24 h and reweighed. Photographs of the film samples were taken to have a qualitative check of the degree of physical degradation in compost as a function of time. The disintegration degree at different days of incubation under compositing conditions was calculated by normalizing the sample weight to the initial weight and the time at which 50% of the material was disintegrated (t_{50}) was estimated by correlating the obtained data with the Boltzmann equation (OriginPro 8.1.software):

$$m = \frac{(m_i - m_\infty)}{1 + e^{(1 - t_{50}/d_t)}} \qquad \text{(Equation 6)}$$

where m_i and m_∞ are the initial and final mass values measured at the beginning of the exposition to compost and after the final asymptotes of the disintegrability test, respectively, while t_{50} is the time at which materials disintegrability reaches the average value between m_i and m_∞, known as the half-maximal degradation, d_t is a parameter that describes the shape of the curve between the upper and lower asymptotes [34]. The disintegration degree at different days of incubation was calculated by normalizing the sample weight to the initial weight and, thus, m_i and m_∞ were set at 0% and 100%, respectively [35].

Structural changes of PU and PU-Cat composites during composting were studied by attenuated total reflectance (ATR) Fourier transformed infrared spectroscopy (FTIR) measurements using a Spectrum One FTIR spectrometer (Perkin Elmer instruments). Spectra were obtained at room temperature in the 4000-650 cm^{-1} region with a resolution of 4 cm^{-1} and 16 scans of accumulation.

2.4. Statistical analysis

Significance in the colorimetric properties and water contact data were statistically analyzed by one-way analysis of variance (ANOVA) using OriginPro 8 software. To identify which groups were significantly different from other groups means comparison were done using the Tukey's test with a 95% confidence level.

3. Results and Discussion

3.1. Synthesis of poly(ester-urethane) and catechin based composites

The expected PCL-middle-block structure in the PLLA-*b*-PCL-*b*-PLLA tri-block copolymer was confirmed by ^{1}H NMR spectroscopy by the presence of PLLA-end groups and the absence of PCL-end groups (see **Fig. S1-a** Supporting Information). The molecular weight, estimated by comparing the ^{1}H NMR signals of protons of PCL and PLLA [27], resulted in 8434,7 g mol^{-1} [11]. Then, the formation of the poly(ester-urethane) was followed by FTIR by checking the disappearance of the stretching vibration of the isocyanate group, –N=C=O at 2270 cm^{-1} (not shown), which confirms the completion of the reaction between the hydroxyl and isocyanate groups after 5h [36]. Additionally, the formation of the urethane bond was confirmed by the ^{1}H NMR spectra by the displacement of the methylene group adjacent to the isocianate group from 3.34 ppm in HDI (peak h in **Fig. 1S-b**) to 3.64 ppm because of the formation of the urethane bond (peak h' **Fig. 1S-c**).

3.2. Visual appearance and optical characterization

The obtained PU and PU-Cat films, with thickness ranging between 195 ± 20 μm, resulted mostly transparent (**Fig. 1A**). However, the presence of catechin reduced the light transmission of the visible region of the spectra, 400-700 nm, as can be seen in **Fig. 1B**. Nevertheless, it should be highlighted that all PU-based materials allow seeing through the films, even those formulations with the highest amount of catechin (5 wt %) (**Fig. 1A-d**), which is one of the most important requirements for the consumers acceptance [37].

It has been reported that catechin had UV-protective action [38], which gain importance in food packaging field to preserve and protect foodstuff from UV radiation until they reach the consumers [4]. Therefore, the ultraviolet light barrier properties of PU based films were investigated in the range of 230-400 nm (**Fig. 1-B**). No significant changes were observed from the visible region of the spectra (400-700 nm) to the UV-A region (315-400 nm), which is the UV sub-region with the lowest energy. Conversely, the addition of catechin into PU matrix shows a positive blocking effect on the UV-B region (280-315 nm) of the spectra, the most energetic component of natural UV light, which causes the most photochemical degradation of plastics [4]. **Fig. 1C** shows the UV-protective action of catechin.

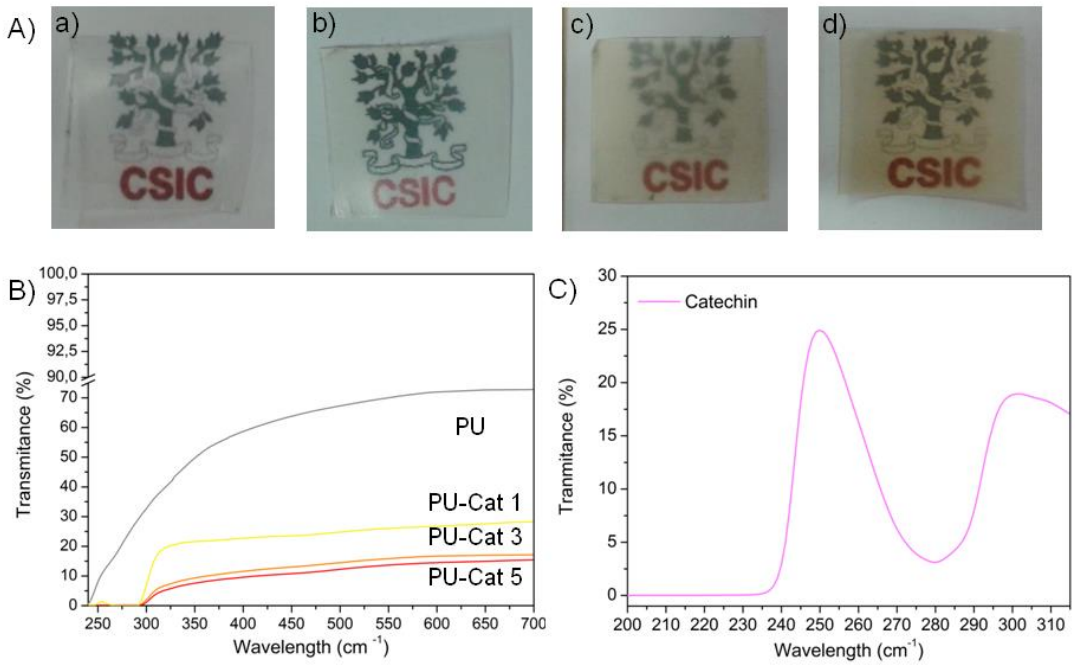

Fig. 1. A) Visual appearance of films: **a)** PU, **b)** PU-Cat1, **c)** PU-Cat3 and **d)** PU-Cat5. **B)** UV-Vis spectra of films and **C)** UV-Vis spectra of catechin (5 10^{-2} mg mL^{-1} in simulant D1).

The color properties were measured in the CIELab space (**Fig. 2**). Neat PU showed the highest lightness value, while PU-Cat5 showed the lowest one in good agreement with the transparency tendency (**Fig. 2-a**). Catechin is a dark orange powder (*L*= 72.7 ± 0.4 a*= 4.3 ± 0.2 and b*= 24.3 ± 0.1) and thus, coordinate a* in films change from small negative values in neat PU to small positive values in PU-Cat5 showing a trend from green (in PU, PU-Cat1 and PU-Cat3) to red (in PU-Cat5) with increasing amount of catechin ($p < 0.05$) (**Fig. 2-b**). In this sense, from the visual appearance of films (**Fig. 1-A**) it was observed that the addition of catechin to the mainly transparent and colorless neat PU resulted in colour changes getting some reddish tone in the PU-Cat5. Catechin presence also produced a stronger tendency towards yellow showing a significant increment in b* ($p < 0.05$) coordinate and in *YI* value ($p < 0.05$). PU-Catechin based materials showed significant total colour differences with respect to neat PU ($p < 0.05$). Moreover, the total colour differences were higher with increasing amount of catechin: ΔE PU-Cat1 = 3.34 ± 0.15, ΔE PU-Cat3 = 11.79 ± 1.09 and ΔE PU-Cat5 = 13.48 ± 1.63. All ΔE values resulted greater than 2.0 in all cases, being this value used as the threshold of perceptible colour difference for the human eye of consumers [39], as it can see from the films appearance in **Fig. 1-A**.

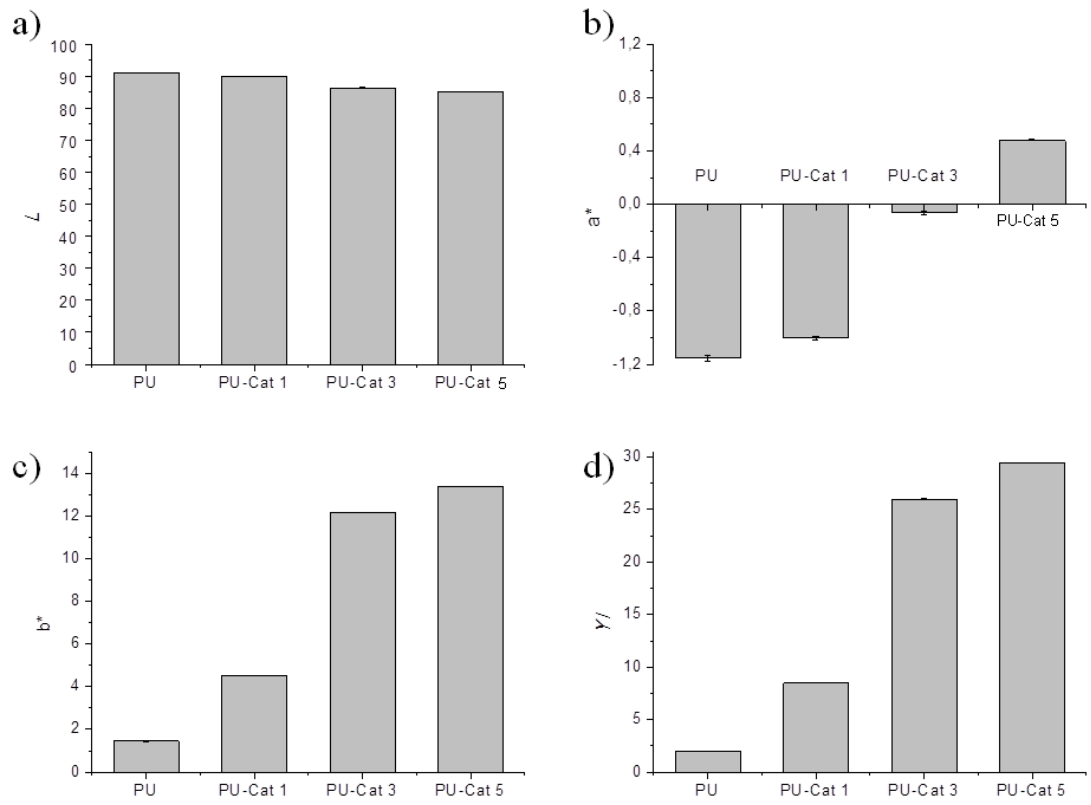

Fig. 2. Colorimetric parameters of PU based films from the CIELab space: **a)** Lightness (*L*) values, **b)** coordinate a*, **c)** coordinate b* and **d)** yellowness index (*YI*).

3.3. Differential scanning calorimetry

The DSC thermogram is shown in **Fig. 3** and the thermal properties are summarizes in Table 1. PLLA block was not able to undergo cold-crystallization in PU and in PU-Cat composites during DSC first heating. Nevertheless, during the second heating, already reported, composites loaded with higher amounts of Cat, PU-Cat3 and PU-Cat5, PCL block cold-crystallized [11]. All PU formulations showed the melting of PCL and PLLA blocks, indicating that the addition of Cat did not avoid the formation of both polymeric crystalline phases during the solvent casting process [9, 11]. The PCL and PLLA degree of crystallinity slightly increased for PU-Cat composites with respect to the neat PU. The endothermic peak of T_m for the PCL is sharper than the PLLA one, which takes place in a large range of temperatures, from about 80 ºC to around 145 ºC [40]. The T_m values of PCL and PLLA blocks were slightly shifted to lower temperatures with the addition of Cat. Similar findings have been obtained in ethylene-vinyl alcohol copolymer with catechin, and the reduction of the melting temperature was ascribed to the antioxidant molecules disrupt the crystal structure, resulting in a

more heterogeneous structure [5]. These DSC results suggest that PU-Cat composites are good candidates for heat-shrinkable packaging films because they are expected to present shape memory properties since both crystalline phases are preserved [13]. In this sense, PCL can act as a switching phase at temperatures close to those required to pack thermally processed food (~ 40 ºC).

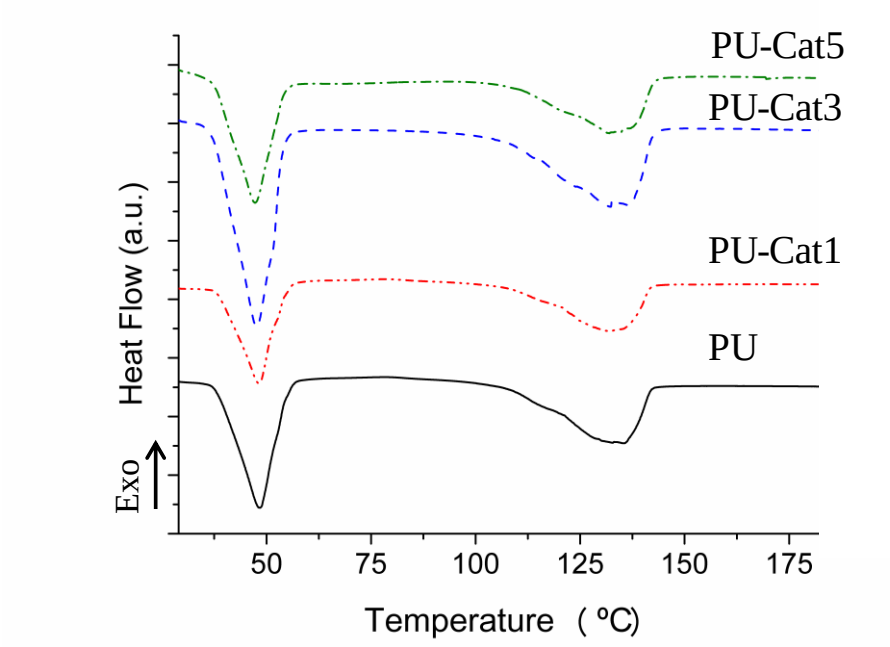

Fig. 3. DSC analysis under nitrogen atmosphere of PU and PU-Cat films (First heating scan).

Table 1. DCS thermal parameters obtained from the first heating scan of PU and PU-Cat composites

Formulation	PCL block			PLLA block		
	T_m (ºC)	ΔH_m (J g^{-1})	X_c (%)	T_m (ºC)	ΔH_m (J g^{-1})	X_c (%)
Neat PU	48.5	20.3	6.9	135.4	20.0	10.9
PU-Cat1	48.2	18.3	6.0	132.3	19.8	10.9
PU-Cat3	47.7	23.0	7.5	132.4	21.6	12.1
PU-Cat5	47.1	19.0	6.3	132.0	18.7	10.7

3.4. Shape memory characterization

It was observed that both crystalline phases of PU are preserved after the incorporation of catechin, suggesting that PU-Cat materials are able to present

thermally-activated shape memory behaviour where the PCL crystalline phase is able to act as a switching phase [9]. Meanwhile, PLLA acts as the fixed phase, responsible to remember the original shape [6]. **Fig. 4-a** shows digital photographs of the visual effect of the complete thermally-activated shape memory cycle for PU-Cat3 as example.

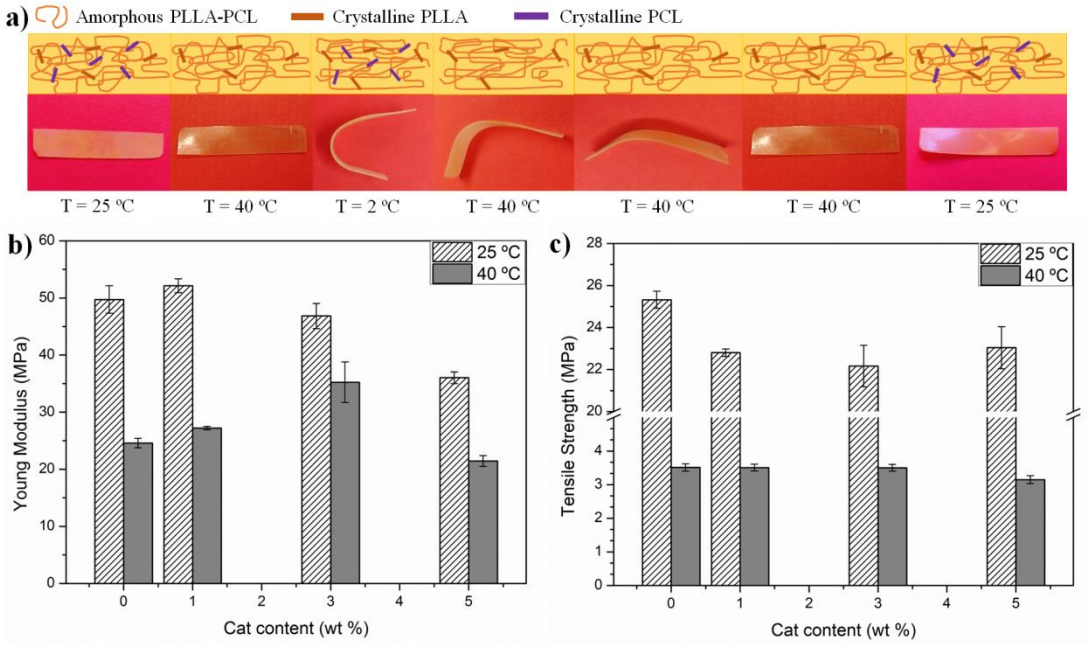

Fig. 4. a) digital photographs of the visual effect of the complete thermally-activated shape memory cycle of PU-Cat3, **b)** Young modulus of PU based films at 25 ºC and 40 ºC and **c)** Tensile strength of PU based materials at 25 ºC and 40 ºC.

Mechanical properties at the T_{trans} were previously studied, in order to know if the materials are able to carry out the thermo-mechanical cycles for the shape-memory characterization. Indeed, when T_{trans} is applied, the switching segment (PCL) starts to melt and the fixed segment (PLLA) is totally responsible for carrying the load [41]. Comparison of the Young modulus and the tensile strength of the PU based materials at two different temperature, at 25 ºC (previously reported) [11] and at 40 ºC, is shown in **Fig. 4.b** and **4.c**, respectively. The Young modulus as well as the tensile strength decreased at higher temperature for all the PU based materials indicating the melting of crystalline PCL. Thus, the obtained results indicated that at 40 ºC, it is possible to perform the thermo-mechanical cycles for the shape-memory characterization. Furthermore, regarding the application of these shape memory PU based materials as heat-shrinkable films for the food packaging field, much easier deformation at high temperature becomes possible at the selected T_{trans}. Therefore, to verify the shape-

memory behavior of the developed materials in a first stage the samples were heated above the melting temperature of PCL, at temperatures close to those required to pack thermally proceeded food (i.e.: 40 ºC) and they were further strained to fix the material in a temporary shape [6]. The temporary shape chosen was 50 % of strain in order to simulate the strain of the films during the packaging process. Subsequently, the films were cooled to 2 ºC simulating the food refrigeration conditions, while maintaining the deformation constant as it will occur during the packed food storage. The applied stress was then removed, and the recovery of the original shape occurs by re-heating the samples again above the T_{trans} [6]. In a second stage, named recovery stage, heating up the material above the transition temperature an increase in the polymer chain mobility is produced, and as a result of the entropy elasticity, the material recovers to its primary shape [15]. The two common representations at 2D and 3D for three thermo-mechanical cycles are shown for PU (2D **Fig. 5-a** and 3D **Fig. 5-c**) and for PU-Cat3 (**Fig. 5-b** and 3D **Fig. 5d**), as examples. In the 2D stress-strain representation, it is possible to calculate the stress variation at ε_m for each cycle, which decreased because of the crystallisation of the PCL switching segments [15]. The stress decreased from a maximum of about 3.6 MPa during the first cycle to 3.4 MPa for the second and the third cycle in neat PU, PU-Cat1 and PU-Cat3. However, the PU-Cat5 showed a lower stress value of 3.3 MPa during the first cycle and it further decreased to 3.1 MPa for the second and the third cycles. The high amount of catechin used in PU-Cat5 composite could not be successfully dispersed and produced some structural defects. The strain fixity ratios were calculated using the Equation 2 as a measure of how well a temporary shape is maintained after removing the applied stress on the sample. An increase of PU strain fixity value was observed with the addition of 1wt% and 3 wt% of catechin (**Fig. 5-e**). Ideally, the fixity would be 100%; however since PLLA is semicrystalline only the crystalline regions are fixing the shape of the materials [15]. In order to verify the fixity of the temporary shape at 2 ºC as a function of the time, the strain values of the deformed samples at free-stress state at 2 ºC were monitored during 24 hours (see **Fig. S2-a** and **S2-b** Supporting Information). During the unloading, there was a part of the material that could not be fixed showing an elastic recovery (i.e.: 7 % and 6 % of the total strain for neat PU and PU-Cat3, respectively). On the contrary, after the elastic recovery, the temporary shape was fixed showing rather constant strain values during 24 hours observing an additional recovery of 3 % after 24 hours at 2 ºC. The enhancement of the fixity of the poly(ester-urethane) matrix at 50 % of strain have been previously

observed by adding cellulose nanocrystals and it was ascribed to the well dispersion of the nanofiller into the PU matrix leading to nanocomposites with higher shape memory properties than the neat PU [9]. However, a decrease of strain fixity ratios occurred in the composite with the highest amount of catechin (PU-Cat5), due to the incomplete catechin dispersion achieved in this sample as it was demonstrated in a previous work by H^1 NMR and scanning electron microscopy (SEM) [11]. In **Fig. 5-g** and **Fig. 5-h** are represented the 2D strain-time diagrams of PU and PU-Cat3 showing that materials are able to recover the original shape in a really short time (5 and 4 minutes for neat PU and PU-Cat3, respectively) when the T_{trans} was applied. Thus, the presence of 3 wt % of Cat leads to an increase of the driving force, responsible to the recovery process. The percentage of recovery, which is related to the ability of the material to recover its initial shape [9], was calculated for all materials using the Equation 3 and the results are shown in **Fig. 5-f**. All PU based formulations showed in the first thermo-mechanical cycle recovery values higher than 94% and during the subsequent thermo-mechanical cycle PU-Cat composites were able to completely recover to the original shapes, while only PU-Ca1 and PU-Cat3 were able to maintain it during the third thermo-mechanical cycle. Therefore, with the addition of low amounts of catechin, that is 1 wt% and 3 wt%, the shape memory parameters of the neat PU matrix were improved, increasing the strain fixity ratio while maintaining constant the excellent strain recovery ratio during the subsequent thermo-mechanical cycles, completely recovering the initial shape. Although some studies with real packed food systems should be done, these materials are interested for smart packaging systems for thermally processed food. In effect, once the food is packed at about 40 ºC the film will achieve a temporary shape that will be retained at the storage temperature of refrigeration. But, if the food loses the cold chain the material will recover its original shape during the heating, leaving an unpacked food as indicator of the cold chain lose.

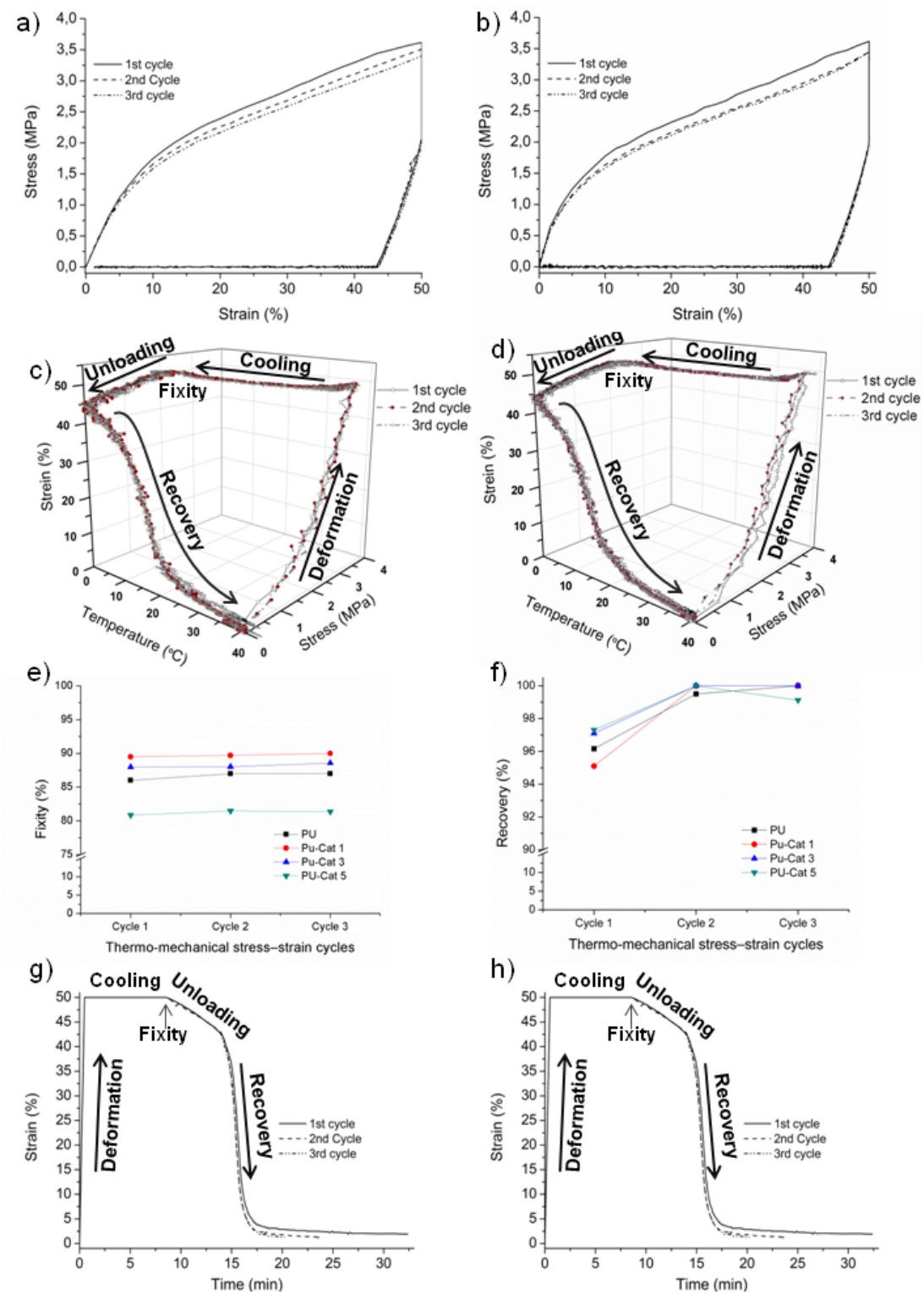

Fig. 5. Thermally-activated shape memory tests of neat PU and PU- Cat3 composite at 50 % of strain: stress-strain diagram 2D representation **a)** PU and **b)** PU- Cat3 and 3D representation **c)** PU and **d)** PU- Cat3.

e) Fixity and **f)** Recovery values of shape memory thermo-mechanical stress-strain cycles of PU and PU-Cat composites.

2D strain-time diagram of **g)** PU and **h)** PU- Cat3.

3.5. Overall and specific migration of catechin

The overall migration of neat PU and the active PU-Cat materials into the food simulant D1 after 10 contact days increased with increasing amount of catechin in the PU formulations (PU= 48 ± 2 mg kg^{-1}, PU-Cat1 = 96 ± 13 mg kg^{-1}, PU-Cat3 = 217 ± 22 mg kg^{-1} and PU-Cat5 = 265 ± 42 mg kg^{-1}), as it is showed in **Fig. 6**. It should be noted that result for neat PU is well below the legal overall migration limit (60 mg kg^{-1} of simulant) [31], while the other formulations exceed this value. Therefore, the specific migration of catechin is required to ensure that the migrated material above the legal limit corresponds to the released catechin. It has been reported that a green tea extract contents approximately 18 mg g^{-1} of catechin, among other antioxidants [32], that is approximately 36 mg of catechin in a cup of green tea (≃180 mg L^{-1}). The release of catechin into the food simulant D1 after 10 contact days increased with increasing amount of catechin in the PU formulation (PU-Cat1 = 70 ± 12 mg kg^{-1}, PU-Cat3 = 207 ± 40 mg kg^{-1} and PU-Cat5 = 232 ± 30 mg kg^{-1}) showing the success of the release capacity of Cat from PU matrix (**Fig. 6**).

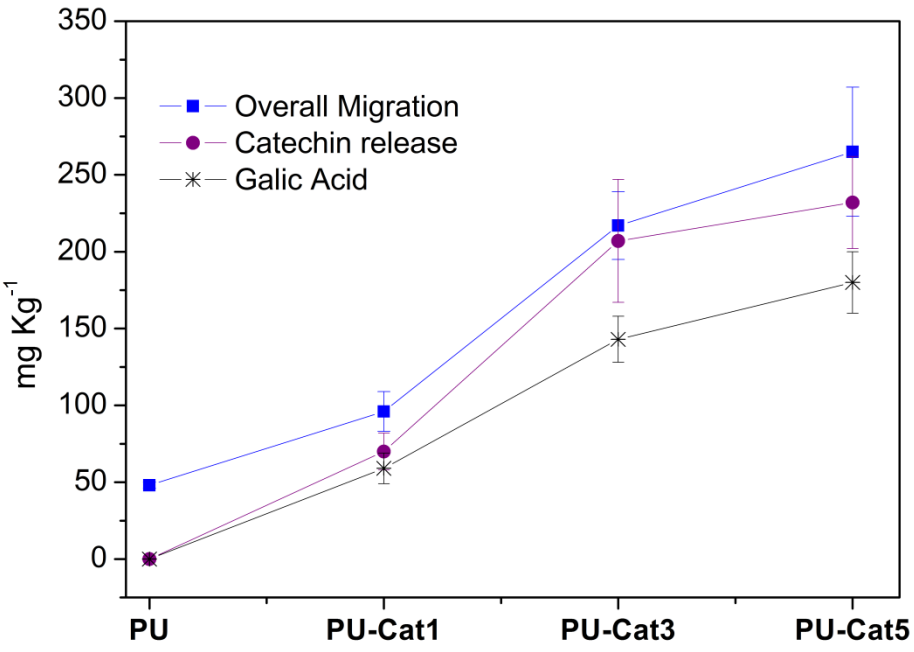

Fig. 6. Overall migration, catechin release and its antioxidant activity expressed as gallic acid concentration measured by DPPH radical scavengers

3.6. Antioxidant activity

The effectiveness of the active PU-Cat as antioxidant packaging materials was demonstrated by the reduction of stable free radical DPPH due to the antioxidant efficacy of catechin presented in the food simulant D1 (**Fig. 6**). The obtained results were expressed as gallic acid (GA) concentration for comparison, being: PU-Cat1 = 59 ± 10 mg kg^{-1}, PU-Cat3 = 143 ± 15 mg kg^{-1} and PU-Cat5 = 180 ± 20 mg kg^{-1}. The antioxidant activity showed comparative tendency to the catechin released from PU matrix showing that the released Cat, which shows high solubility in ethanol (50 g L^{-1}), is able to interact with fatty food protecting them from oxidative process and extending their shelf-life. In a previous work biodegradable materials based on PLA-PHB blends incorporated with 5 wt% of catechin showed similar antioxidant activity, but those materials required the addition of a plasticizer to improve the release of catechin [24].

3.7. Water contact angle measurements

Water contact angle measurements are usually measured in materials for food packaging application to evaluate the hydrophilic/hydrophobic character of the materials since they are required to protect food stuff from humidity during transport, handling and storage [42]. In fact, one drawback of PLA-based materials for the food packaging industry is that it presents a higher natural hydrophilicity than conventional thermoplastic polymers frequently used as food packaging [43]. It should be highlighted that all formulations showed water contact angle values higher than 65º (Table 2), showing their hydrophobic surface, highlighting their potential use for food packaging applications [44]. The PU added with 1 wt% and 3 wt% of catechin composites resulted in films with higher water contact angles, and thus with a surface hydrophobicity increased ($p < 0.05$). The positive effect of catechin presence in the wettability of PU-Cat composites could be due to the film surfaces chemical and topographical properties changes due to the catechin microparticles presence. In this sense, hydrogen bonding interactions between catechin hydroxyl groups with carbonyl groups of PCL and PLLA can be formed, and therefore, catechin hydroxyl groups did not show surface orientation being less available to interact with water at their surface. Similar findings have been previously observed in PLA-based materials loaded with catechin [24, 45]. Conversely, PU-Cat5 was the more hydrophilic composite, probably due to the presence of higher amounts of available catechin hydroxyl groups to interact with water at the surface as a

result of the non-well dispersed catechin into PU matrix. In fact, catechin aggregates were observed in PU-Cat5 [11], which are more susceptible to interact with water.

Table 2. Water contact angle measurements, time at which 50% of PU and active PU-Cat composites were degraded under composting conditions and the corresponding correlation coefficients between theoretical and experimental data (R^2).

Film formulations	θ^o	t_{50} (day)	R^2
PU	71.5 ± 0.3^a	35.8	0.994
PU-Cat1	75.1 ± 2.9^b	31.9	0.983
PU-Cat3	77.8 ± 1.5^b	35.6	0.988
PU-Cat5	72.2 ± 1.5^a	28.0	0.987

[a-b] Different superscripts within the θ^o values indicate significant differences between formulations ($p < 0.05$).

3.8. Disintegration under composting conditions

The compostability attribute of biodegradable materials has gained considerable attention for short term food packaging applications mainly because of recycling is energy expensive and requires additional washing steps, while composting allows disposal of the packages in compost where the plastic material undergoes degradation by biological processes yielding to carbon dioxide and water, living no visually distinguishable materials [46]. Therefore, the disintegrability was conducted to corroborate the biodisintegrable character of all PU and active PU-Cat based composites. In **Fig. 7** are shown the visual appearance of films during the disintegration in composting conditions, confirming the biodegradable character of all the formulations studied. During the initial period of the disintegration (9 days, **Fig. 7-a**) films become breakable and opaque as a consequence of the changes in the polymer matrices refraction index due to the water absorption and/or presence of products formed by the hydrolytic degradation process [47]. The films disintegrability was also quantified in terms of mass loss as a function of composting time (**Fig. 7-b**) using the Boltzman equation [35]. The estimated regression parameters of the fitted results of the non-linear model as well as the t_{50} were calculated (Table 2), while m_i and m_∞ values were assigned as 0% and 100% of disintegrability, respectively. The correlation coefficients between theoretical and experimental data (R^2) resulted higher than 0.980

for all composites, suggesting only minor differences in the fitting of the model to experimental values. Catechin presence speeds up the disintegration of PU as it occurred in PLA-PHB blends loaded with catechin [45]. The PLA and PCL disintegration in compost starts by a hydrolytic degradation due to water absorption followed by the polymer chain broken [48]. Thus, it is expected that the more hydrophilic surfaces will be earlier disintegrated. In fact, we recently studied the hydrolytic degradation of PU-nanohydroxyapatite nanocomposites in a phosphate buffer solution at 37 ºC, and the degradation results were in agreement with surface hydrophilicity [7]. In the present research the neat PU showed the lowest disintegration rate with the lowest half-maximal degradation (t_{50}), even though it presents the more hydrophilic surface, as it revealed the lower water contact angle measurements. This unexpected result could be related with the fact that during the composting test the materials are continuously exposed to temperatures at which the PCL block is above the melt state (58 ºC), leading to an increase on the polymer chain mobility which facilitates the water penetration and PU loaded with catechin, which presents high amount of OH-groups, become more susceptible to water attack. Accordingly, the higher disintegration rate was observed for PU-Cat5. Other than PU-Cat1 showed higher disintegration rate than PU-Cat3, which actually did not significantly shift the half maximum degradation rate of neat PU. It should be highlighted that the second step of the disintegration process is governed by the microorganisms enzymatic attack [48], where the highest crystallinity of PLLA block developed in PU-Cat3 composite due to the catechin nucleating effect is delaying the action of microorganisms in the composting medium. Finally, some colour changes of the compost medium were observed (not shown) due to the aerobic fermentation that results in dark humus soil.

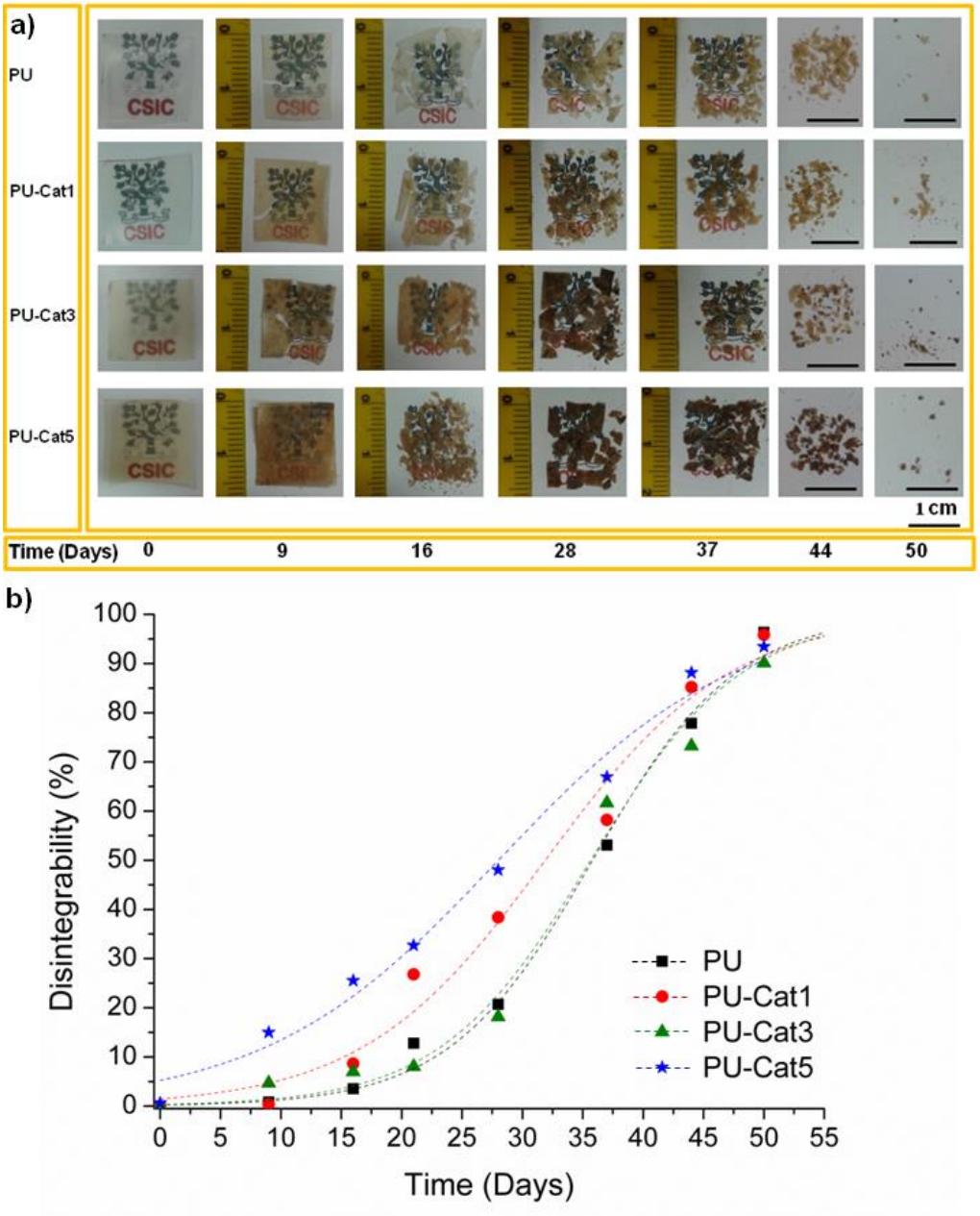

Fig. 7. Disintegrability under composting conditions of PU and PU-Cat composite films: **a)** Visual appearance before and after different incubation days, **b)** films disintegration degree (%) as a function of time.

The structural changes during the composting process were followed by FTIR analysis and the FTIR spectra at different days of disintegration are presented in **Fig. 8** for neat PU (**Fig. 8-a**) and for PU-Cat1 composite (**Fig. 8-b**) as an example. The disintegration process affected the urethane bond decreasing the peak intensity of NH bending at 1536 cm^{-1}, as it occurred with neat PU degradation in a phosphate buffer solution [7]. For neat PU (**Fig. 8-a**), these band practically disappeared in 28 days,

while at that time also appeared a broad band in the region between 1550 and 1650 cm^{-1} related to the formation of carboxylate ions during the disintegration process [49, 50]. In the case of catechin loaded samples it was observed that the relationship between the intensity of the peak corresponding to the stretching vibrations of the C=C group of the catechin aromatic ring at 1620 cm^{-1} with the intensity of the peak of the NH bending increased as a consequence of the disintegration of PU matrix after 9 days of disintegration (**Fig. 8-b**). After 16 days of disintegration the NH bending of PU-Cat1 (**Fig. 8-b**) seems to be lower than the same band in neat PU sample (**Fig. 8-a**), attributable to the accelerating effect of catechin on the disintegration process.

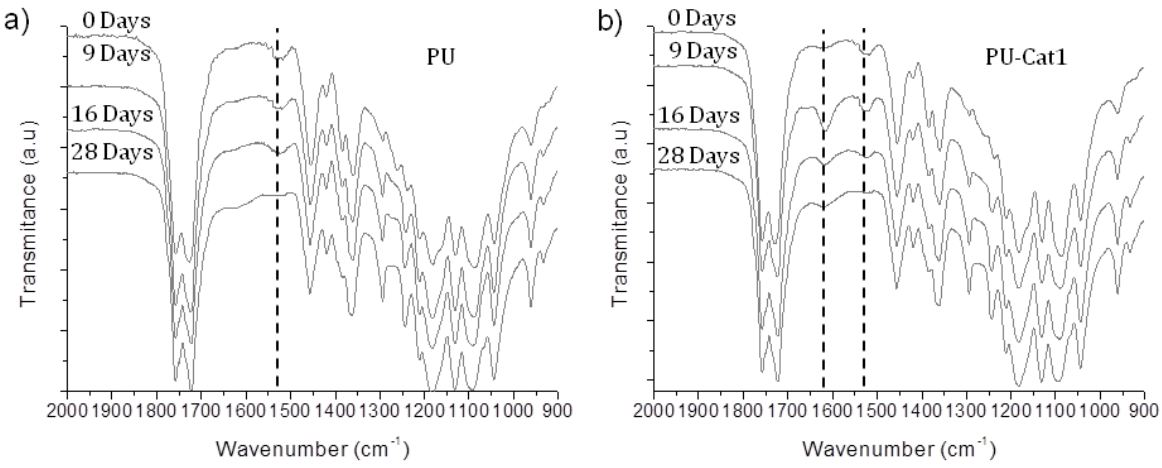

Fig.8. FTIR spectra (2000 - 900cm^{-1}) at different disintegration times under composting conditions of: **a)** PU and **b)** PU-Cat1.

4. Conclusions

Antioxidant poly(ester-urethane) based composites were successfully developed by incorporating different amounts of catechin to a PU matrix based on PLLA and PCL block copolymer structure. PU films maintained their transparency after the addition of the natural antioxidant, but thus increasing the amount of catechin a stronger yellow tendency was observed, up to reaching a reddish tone in PU-Cat5. In general, Cat slightly increased the crystallinity of PU, particularly in the case of PU-Cat3 where both PCL and PLLA blocks showed an increment of the crystallinity. These smart PU-based materials were thermally activated at temperatures at which the processed food is frequently packed (i.e.: 40 ºC). PU-based materials with catechin in low amounts, 1 wt% and 3 wt%, showed an improvement on the strain fixity ratio on the shape memory behavior of neat PU and allowed to completely recover the initial shape maintaining

constant the strain recovery ratio at 100%. The improvement in the shape memory behaviour in PU-Cat1 and PU-Cat3 can be mainly ascribed to the positive interactions between the antioxidant and the poly(ester-urethane) matrix. Neat PU showed overall migration values well below the legislation limits in a fatty food simulant. Catechin was effectively released from PU matrix and its inherent antioxidant activity was maintained in the food simulant, while it resulted proportional to the antioxidant released. Well dispersed catechin in PU matrix were able to better interact with the polymer matrix increasing the polymer-catechin microparticle interfacial adhesion, leading to a decrease of the surface adhesive forces improving the water resistance. All PU-based formulations were successfully disintegrated under composting medium in less than two months, stating their compostable character. Catechin presence speeds up the disintegration process of PU matrix in compost. Therefore, it is possible to conclude that the synthesized transparent poly(ester-urethane)s based on PLLA and PCL incorporated with low amounts, 1 wt % and 3 wt %, of catechin showed their potential as active heat-shrinkable advanced films for biodegradable food packaging applications.

Acknowledgements

Authors thank Spanish Ministry of Economy and Competitiveness, MINECO, (MAT2013-48059-C2-1-R) and Regional Government of Madrid (S2013/MIT-2862) for the financial support. M.P.A. and L.P. acknowledge the Juan de la Cierva (FJCI-2014-20630) and Ramon y Cajal (RYC-2014-15595) contracts from the MINECO, respectively. Authors also thank Prof. Juan López Martínez (Universitat Politècnica de València, Spain) for his assistance in colourimetric and water contact angle measurements as well as Dr. Carolina López de Dicastillo (Universidad de Santiago de Chile) for her assistance with catechin powder colourimetric measurements.

References

[1] Etxabide A, Uranga J, Guerrero P, de la Caba K. Development of active gelatin films by means of valorisation of food processing waste: A review. Food Hydrocolloids. 2016.

[2] Rhim J-W, Park H-M, Ha C-S. Bio-nanocomposites for food packaging applications. Progress in Polymer Science. 2013;38(10–11):1629-1652.

[3] Arrieta MP, Peltzer MA, Garrigós MDC, Jiménez A. Structure and mechanical properties of sodium and calcium caseinate edible active films with carvacrol. Journal of Food Engineering. 2013;114(4):486-494.

[4] Auras R, Harte B, Selke S. An overview of polylactides as packaging materials. Macromolecular Bioscience. 2004;4(9):835-864.

[5] Raquez JM, Habibi Y, Murariu M, Dubois P. Polylactide (PLA)-based nanocomposites. Progress in Polymer Science. 2013;38(10-11):1504-1542.

[6] Peponi L, Navarro-Baena I, Sonseca A, Gimenez E, Marcos-Fernandez A, Kenny JM. Synthesis and characterization of PCL-PLLA polyurethane with shape memory behavior. European Polymer Journal. 2013;49(4):893-903.

[7] Navarro-Baena I, Arrieta MP, Sonseca A, Torre L, López D, Giménez E, et al. Biodegradable nanocomposites based on poly(ester-urethane) and nanosized hydroxyapatite: Plastificant and reinforcement effects. Polymer Degradation and Stability. 2015;121:171-179.

[8] Navarro-Baena I, Kenny JM, Peponi L. Crystallization and thermal characterization of biodegradable tri-block copolymers and poly(ester-urethane)s based on PCL and PLLA. Polymer Degradation and Stability. 2014;108:140-150.

[9] Navarro-Baena I, Kenny JM, Peponi L. Thermally-activated shape memory behaviour of bionanocomposites reinforced with cellulose nanocrystals. Cellulose. 2014;21(6):4231-4246.

[10] Soman S, Chacko AS, Prasad VS. Semi-interpenetrating network composites of poly(lactic acid) with cis-9-octadecenylamine modified cellulose-nanofibers from Areca catechu husk. Composites Science and Technology. 2017;141:65-73.

[11] Arrieta MP, Peponi L. Polyurethane based on PLA and PCL incorporated with catechin: Structural, thermal and mechanical characterization. European Polymer Journal. 2017;89:174-184.

[12] Saralegi A, Gonzalez ML, Valea A, Eceiza A, Corcuera MA. The role of cellulose nanocrystals in the improvement of the shape-memory properties of castor oil-based segmented thermoplastic polyurethanes. Composites Science and Technology. 2014;92:27-33.

[13] Peponi L, Navarro-Baena I, Kenny JM. Shape memory polymers: Properties, synthesis and applications. Smart Polymers and their Applications2014. p. 204-236.

[14] Sessini V, Raquez JM, Lo Re G, Mincheva R, Kenny JM, Dubois P, et al. Multiresponsive Shape Memory Blends and Nanocomposites Based on Starch. ACS Applied Materials and Interfaces. 2016;8(30):19197-19201.

[15] D'Hollander S, Van Assche G, Van Mele B, Du Prez F. Novel synthetic strategy toward shape memory polyurethanes with a well-defined switching temperature. Polymer. 2009;50(19):4447-4454.

[16] Raquez JM, Vanderstappen S, Meyer F, Verge P, Alexandre M, Thomassin JM, et al. Design of cross-linked semicrystalline poly(ε-caprolactone)-based networks with one-way and two-way shape-memory properties through Diels-Alder reactions. Chemistry - A European Journal. 2011;17(36):10135-10143.

[17] Peponi L, Arrieta MP, Mujica-Garcia A, López D. Smart Polymers. In: Jasso-Gastinel C, Kenny JM, editors. Modification of Polymers Properties. Guadalajara, México: ELSEVIER; 2017. p. 131-154.

[18] Morshedian J, Khonakdar HA, Mehrabzadeh M, Eslami H. Preparation and properties of heat-shrinkable cross-linked low-density polyethylene. Advances in Polymer Technology. 2003;22(2):112-119.

[19] Behl M, Razzaq MY, Lendlein A. Multifunctional Shape-Memory Polymers. Advanced Materials. 2010;22(31):3388-3410.

[20] Gaze J. Microbiological aspects of thermally processed foods. Journal of applied microbiology. 2005;98(6):1381-1386.

[21] Dainelli D, Gontard N, Spyropoulos D, Zondervan-van den Beuken E, Tobback P. Active and intelligent food packaging: legal aspects and safety concerns. Trends in Food Science & Technology. 2008;19, Supplement 1:S103-S112.

[22] Vanderroost M, Ragaert P, Devlieghere F, De Meulenaer B. Intelligent food packaging: The next generation. Trends in Food Science and Technology. 2014;39(1):47-62.

[23] Fernández-Pan I, Royo M, Ignacio Maté J. Antimicrobial Activity of Whey Protein Isolate Edible Films with Essential Oils against Food Spoilers and Foodborne Pathogens. Journal of Food Science. 2012;77(7):M383-M390.

[24] Arrieta MP, Castro-López MDM, Rayón E, Barral-Losada LF, López-Vilariño JM, López J, et al. Plasticized poly(lactic acid)-poly(hydroxybutyrate) (PLA-PHB) blends incorporated with catechin intended for active food-packaging applications. Journal of Agricultural and Food Chemistry. 2014;62(41):10170-10180.

[25] López De Dicastillo C, Castro-López MDM, Lasagabaster A, López-Vilariño JM, González-Rodríguez MV. Interaction and release of catechin from anhydride maleic-grafted polypropylene films. ACS Applied Materials and Interfaces. 2013;5(8):3281-3289.

[26] Sessini V, Arrieta MP, Kenny JM, Peponi L. Processing of edible films based on nanoreinforced gelatinized starch. Polymer Degradation and Stability. 2016;132:157-168.

[27] Navarro-Baena I, Marcos-Fernández A, Fernández-Torres A, Kenny JM, Peponi L. Synthesis of PLLA-b-PCL-b-PLLA linear tri-block copolymers and their corresponding poly(ester-urethane)s: Effect of the molecular weight on their crystallisation and mechanical properties. RSC Advances. 2014;4(17):8510-8524.

[28] Fombuena V, Balart J, Boronat T, Sánchez-Nácher L, Garcia-Sanoguera D. Improving mechanical performance of thermoplastic adhesion joints by atmospheric plasma. Materials and Design. 2013;47:49-56.

[29] Turner JF, Riga A, O'Connor A, Zhang J, Collis J. Characterization of drawn and undrawn poly-L-lactide films by differential scanning calorimetry. Journal of Thermal Analysis and Calorimetry. 2004;75(1):257-268.

[30] Peponi L, Navarro-Baena I, Báez JE, Kenny JM, Marcos-Fernández A. Effect of the molecular weight on the crystallinity of PCL-b-PLLA di-block copolymers. Polymer (United Kingdom). 2012;53(21):4561-4568.

[31] European Commission. No. 10/2011 of 14 January 2011 on plastic materials and articles intended to come into contact with food. Official Journal of European Union. 2011;L12:1−89.

[32] Castro López MDM, De Dicastillo CL, Vilariño JML, Rodríguez MVG. Improving the capacity of polypropylene to be used in antioxidant active films: Incorporation of plasticizer and natural antioxidants. Journal of Agricultural and Food Chemistry. 2013;61(35):8462-8470.

[33] UNE EN ISO. Determination of the degree of disintegration of plastic materials under simulated composting conditions in a laboratory-scale test. 202002016.

[34] Arrieta MP, Parres F, López J, Jiménez A. Development of a novel pyrolysis-gas chromatography/mass spectrometry method for the analysis of poly(lactic acid) thermal degradation products. Journal of Analytical and Applied Pyrolysis. 2013;101:150-155.

[35] Arrieta MP, Fortunati E, Dominici F, López J, Kenny JM. Bionanocomposite films based on plasticized PLA–PHB/cellulose nanocrystal blends. Carbohydrate Polymers. 2015;121:265-275.

[36] Barrera-Rivera KA, Peponi L, Marcos-Fernández Á, Kenny JM, Martínez-Richa A. Synthesis, characterization and hydrolytic degradation of polyester-urethanes obtained by lipase biocatalysis. Polymer Degradation and Stability. 2014;108:188-194.

[37] Arrieta MP, López J, Ferrándiz S, Peltzer MA. Characterization of PLA-limonene blends for food packaging applications. Polymer Testing. 2013;32(4):760-768.

[38] Yoshino S, Mitoma T, Tsuruta K, Todo H, Sugibayashi K. Effect of emulsification on the skin permeation and UV protection of catechin. Pharmaceutical Development and Technology. 2013;19(4):395-400.

[39] Arrieta MP, Peltzer MA, López J, Garrigós MDC, Valente AJM, Jiménez A. Functional properties of sodium and calcium caseinate antimicrobial active films containing carvacrol. Journal of Food Engineering. 2014;121(1):94-101.

[40] Navarro-Baena I, Arrieta MP, Mujica-Garcia A, Sessini V, Lopez D, Kenny JM, et al. Thermal Degradation Effects on Polyurethanes and Their Nanocomposites. Reactions and Mechanisms in Thermal Analysis of Advanced Materials2015. p. 165-189.

[41] Kim BK, Lee SY, Xu M. Polyurethanes having shape memory effects. Polymer. 1996;37(26):5781-5793.

[42] Arrieta MP, Fortunati E, Dominici F, Rayón E, López J, Kenny JM. PLA-PHB/cellulose based films: Mechanical, barrier and disintegration properties. Polymer Degradation and Stability. 2014;107:139-149.

[43] Quirós J, Boltes K, Aguado S, de Villoria RG, Vilatela JJ, Rosal R. Antimicrobial metal-organic frameworks incorporated into electrospun fibers. Chemical Engineering Journal. 2015;262:189-197.

[44] Hambleton A, Fabra M-J, Debeaufort F, Dury-Brun C, Voilley A. Interface and aroma barrier properties of iota-carrageenan emulsion–based films used for encapsulation of active food compounds. Journal of Food Engineering. 2009;93(1):80-88.

[45] Arrieta MP, López J, López D, Kenny JM, Peponi L. Effect of chitosan and catechin addition on the structural, thermal, mechanical and disintegration

properties of plasticized electrospun PLA-PHB biocomposites. Polymer Degradation and Stability. 2016;132:145-156.

[46] Kale G, Kijchavengkul T, Auras R, Rubino M, Selke SE, Singh SP. Compostability of bioplastic packaging materials: An overview. Macromolecular Bioscience. 2007;7(3):255-277.

[47] Fortunati E, Puglia D, Santulli C, Sarasini F, Kenny JM. Biodegradation of Phormium tenax/poly(lactic acid) composites. Journal of Applied Polymer Science. 2012;125(SUPPL. 2):E562-E572.

[48] Kale G, Auras R, Singh SP. Comparison of the degradability of poly(lactide) packages in composting and ambient exposure conditions. Packaging Technology and Science. 2007;20(1):49-70.

[49] Fortunati E, Armentano I, Iannoni A, Barbale M, Zaccheo S, Scavone M, et al. New multifunctional poly(lactide acid) composites: Mechanical, antibacterial, and degradation properties. Journal of Applied Polymer Science. 2012;124(1):87-98.

[50] Arrieta MP, López J, Rayón E, Jiménez A. Disintegrability under composting conditions of plasticized PLA–PHB blends. Polymer Degradation and Stability. 2014;108:307-318.